

THREE DIMENSIONAL SEGMENTATION OF OPTICAL MICROSCOPE IMAGES.

M. Razaz, J. A. Bangham, R. A. Lee and R. W. Harvey

School of Information Systems
University of East Anglia
Norwich England

Email : mr@sys.uea.ac.uk

ABSTRACT

Three dimensional optical microscopy images are noisy and blurred, have nonuniform background, and contain objects which do not usually have sharp edges or may have noise induced boundaries. As a result, traditional segmentation techniques are not suitable for this type of applications. We present a novel methodology based on a combination of 3D nonlinear restoration and morphological sieving which can be used to successfully segment 3D optical microscopy images. The nonlinear restoration removes the blur and noise aberrations from such real images and the sieve algorithm segments out their subcellular features. The methodology is discussed and experimental results using both synthetic and real 3D images are presented.

There is little work in the literature on automatic segmentation of optical microscopy images. The need for efficient and reliable methods to automatically recognise 3D objects in such vast image data sets, followed by features extraction, is overdue. Traditional segmentation techniques such as edge detection, thresholding, amplitude projection, split and merge, etc. [16] would not be able to deal with such real 3D images; the background is not uniform, nuclei may have different average luminance and their edges may not be sharp, and false noise-induced edges may be present. As a result, for example by using edge detection/thresholding techniques, typically many features present in an observed image may be lost in the resulting segmented image. We present a novel combination of nonlinear image restoration [3,4,7] and the Sieve algorithm [10,11] for segmenting such images. The nonlinear restoration first removes intelligently the noise and blur from the image, and the Sieve algorithm then segments out subcellular features in the restored image.

1. INTRODUCTION

Three dimensional (3D) imaging systems are becoming more widespread. Confocal laser scanning microscopes are used, for example, in a variety of biological and biomedical applications. We use confocal imaging, in collaboration with other research institutes, to study various cellular structures and processes in plants. Particular components within cells, for instance specific genes or proteins, are labelled by florescent probes. Focal sectioning is then applied to generate three dimensional images of the sub-cellular structures. Vast amount of image data is thus generated; typically between 60 to 90 optical sections of 512x512 pixels each. These images are subject to a number of distortions. In particular they are noisy, and invariably blurred by the point spread function (PSF) of the imaging system. The PSF can be experimentally determined, and then modelled [5].

2. 3D SEGMENTATION METHODOLOGY

The restoration of 3D optical microscopy images by traditional linear techniques [16] produces poor quality images that are often marred by artefacts such as oscillations or 'ringing' around sharp changes in intensity in the image, negative pixel values, etc [3]. This is because the restoration process is a difficult ill-posed mathematical problem with many feasible solutions and hence it has to be regularised by incorporating in the problem formulation *a priori* knowledge in the form of constraints for restricting the set of admissible solutions [1,2]. We have developed new nonlinear restoration methods using constrained iterative deconvolution and projection onto convex sets (POCS) methods [3, 4, 5, 6, 7] which overcome these

difficulties and produce significantly enhanced images in terms of signal to noise ratio and resolution.

A consequence of image restoration is that “granular” noise may become more visible, mainly in the background, and the intensity changes steeper at feature boundaries within a confocal image. It is appropriate to segment images with these characteristics using methods based on mathematical morphology.

It is common for biological structures to have characteristic volumes but very variable shapes. For example, liver and pancreas have variable shape but more constant relative volume (weight), and volume has long been used to characterise red blood cells. Similarly subcellular organelles are often distinguishable by volume rather than shape.

We have used a multidimensional Sieve algorithm [10, 11, 14] to segment restored images, and remove small-scale noise granules. The connected sieves used do not introduce new features in the restored image and are capable of discriminating effectively between objects of different volumes, for example irregular shaped subcellular organelles, in a particular range of volumes, are clearly distinguished without distorting their shape.

2.1 3D Nonlinear Restoration

Two nonlinear algorithms were developed for restoration of 3D optical microscopy images [3,7] These are the constrained iterative deconvolution algorithm (IDA) and the POCS method. Both methods incorporate constraints in order to regularise the ill-conditioned restoration problems. The details of IDA are described in [3], and we briefly discuss here the POCS method.

In the POCS approach [7], each constraint forms a closed convex set onto which a solution is projected. The overall solution lies in the intersection of these sets. For n constraints, there are n sets and the solution ought to lie in the intersection

$$\zeta_0 = \bigcap_{i=1}^n \zeta_i; \quad i = 1, 2, 3, \dots, n$$

A solution in ζ_0 will satisfy all the constraints, and is unique if ζ_0 contains a single point. On the other hand if ζ_0 is empty, there does not exist any solution; which may correspond to wrong constraints or noisy image data. Assuming P_i and P_0 to be the orthogonal projection operators of g onto ζ_i and ζ_0 , and T_i

$$T_i = 1 + \beta_i (P_i - 1)$$

where $\{\beta_i\}$ are relaxation parameters, $0 < \beta_i < 2$. g is a fixed point of P_0 and P_i , and hence of T_i and of the composite operator, $T = T_n T_{n-1} \dots T_1$, then the POCS algorithm is given by $g_{k+i} = T g_k$. The sequence $\{g_k\}$ converges weakly to a fixed point of ζ_0 provided the

latter is a nonempty set. g_0 is an arbitrary initial guess. If the relaxation parameter $\beta_i = 1$, then this equation reduces to

$$g_{k+1} = P g_k,$$

where $P = P_n P_{n-1} \dots P_1$. The constraints are: the source is positive, an upper bound on the noise variance, band-limitedness and energy boundedness.

2.2 The Sieve

This is a morphological transform which preserves scale-space and can operate in multiple dimensions [10-14]. The Sieve functions by removing extrema of successively increasing size. Sieves can be considered as a special class of alternating sequential filters operating on connected sets [8, 9], and are particularly effective at rejecting impulsive granular noise. Very sharp edged objects are handled well by sieves, but smoothly changing objects are less well handled because they spread over many scales in the granularity domain. This is the converse of the case with linear filters that spread edges over many scales or frequencies.

A connected set sieve in N dimensions $\Phi_m: Z^N \rightarrow Z^N$ operates on graphs [15]. An image can be described by a connected graph, $H=(V,E)$ where V is the set of vertices and E the set of edges. Let $C_r(H)$ denote the set of connected subsets, when $N=2$ these represent areas and when $N=3$, volumes.

$$\Phi_m(X) = \phi(\Phi_{m-1}(X)), \quad \text{where } \Phi_0(X) = X$$

The operator ϕ_m may be an open/close (M -sieve) $\max(\min(\min(\max(C_r(H)))))$ or area close/open (N -sieve) $\min(\max(\max(\min(C_r(H)))))$ or a recursive equivalent, each operating on graphs with a set of connected subsets with m elements. It is emphasised that ϕ_m operates on connected sets without regard to shape and there is no structuring element. The differences between successive images in the decomposition are the granule functions

$$Gran_R(X)(m) = (R_m(X)) - (R_{m+1}(X))$$

The set of granules $\{G\}$ represent the non-zero intervals in the granule functions characterised by the triplet {width, amplitude and position} and the sieve transform maps the signal into a set of granules. Objects that have volumes lying in the range, m_1 to m_2 , are preserved by adding together the granule functions in that range and the process rejects objects of larger and smaller volume.

2. RESULTS

Images of pea root cells that have been labelled with a fluorescent probe are observed with a scanning confocal microscope. The label allows the nucleolus and associated structures to be seen. The PSF for the entire system is obtained by imaging a subresolution fluorescent bead and fitting a bicubic spline to the experimental data set [5]. This modelled PSF is then used to restore the 3D image data sets of the root cells to yield an estimate of the source function. Once the image is restored, it is then Sieved to identify its subcellular features.

We present here typical experimental results for both synthetic and real images. The first example (see Figures 1 and 2) is a 3D synthetic image which has been blurred and then Gaussian noise added to it. Figure 1 shows a single section of the 3D synthetic image which has been restored and then segmented by the Sieve. Figures 2a is the blurred and noisy original 3D image after being rendered by the Iris Explorer visualisation tools. Figures 2b and 2c show the corresponding restored and segmented images in 3D, respectively. Notice that very small-scale noise granules are generated mainly in the background region of the image. As can be seen our methodology based on nonlinear restoration and sieving has

effectively recognised all the different 3D objects in the image, despite their varying size and shape.

The second example is the 3D image of a pea root nucleolus obtained from the confocal microscope operated at the limits of the resolution by near ultra-violet light (see Figures 3 and 4). Figure 3a shows a single 2D image slice (out of 60 slices altogether) which is blurred as result of the optical PSF, and is also noisy. Figures 3b and 3c show respectively the restored and sieved versions of the single image slice in Figure 3a.

Figure 4a shows the entire observed image data after volume rendering by the Iris Explorer. The blurred edges of the fluorescently labelled objects and the background large scale intensity changes make it difficult to select a satisfactory threshold above which the Explorer will render objects as solids. Figures 4b show the same data in Figure 4a after 3D nonlinear restoration. The image has clearly been sharpened but now the features of interest need to be separated from both the background and very small-scale granular noise. The application of a 3D sieve tuned to distinguish the range of volumes of interest makes it easier to interpret the image (see Figure 4c).

Figures 5 and 6 show the results of applying our segmentation methodology to another confocal image data set. All the observations made previously for Figures 3 and 4 are also applicable here.

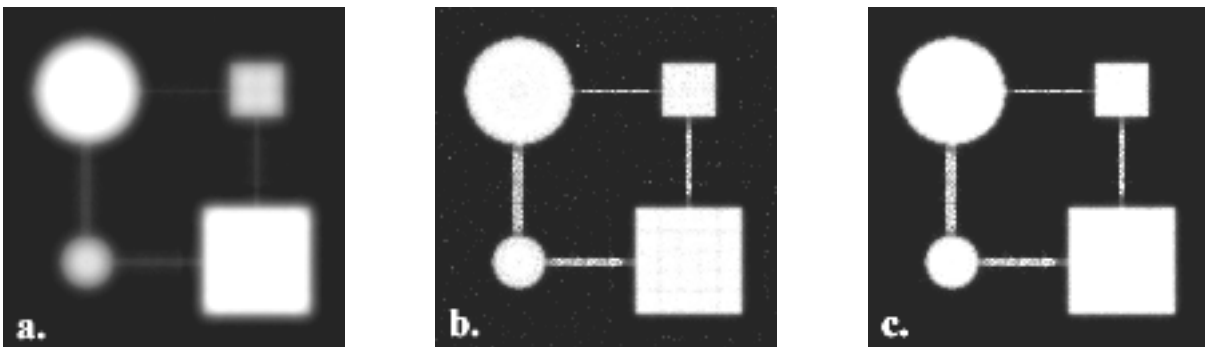


Figure 1. Restoration and segmentation of a single 2D slice from a 3D blurred and noisy synthetic image. Picture a- A single slice from the original image set, Picture b- Image in (a) after nonlinear restoration, and Picture c- Image in (b) after segmentation by the sieve.

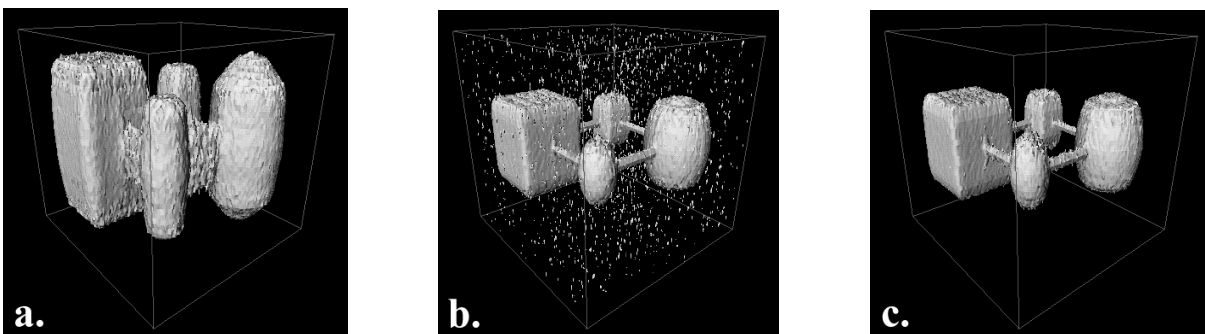


Figure 2. 3D Restoration and segmentation of a blurred and noisy synthetic image. Picture a- the blurred and noisy original image data after being rendered by Iris Explorer, Picture b- the original image in (a) after nonlinear restoration, and Picture c- image in (b) after segmentation by Sieve.

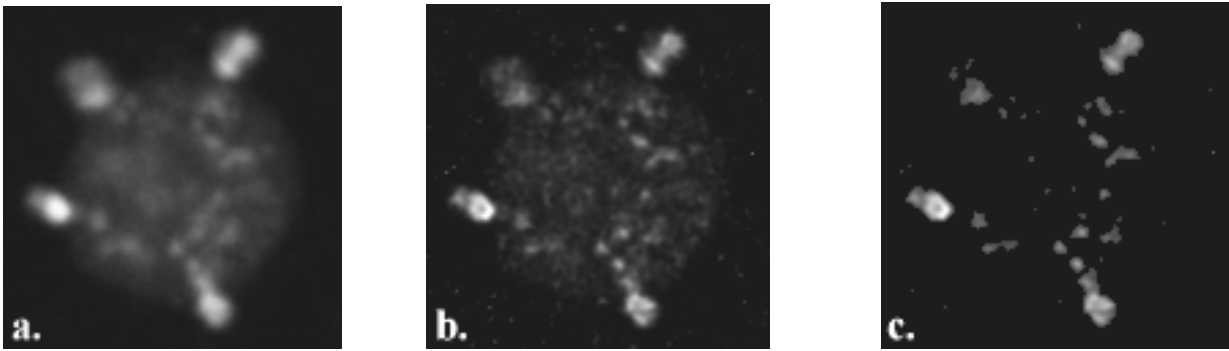


Figure 3. Restoration and segmentation of a single 2D slice from an original 3D confocal image data set of 60 x128x128 voxels. Picture a - A single image slice of 128x128 pixels, Picture b - image (a) after nonlinear restoration, and Picture c- image (b) after segmentation by the Sieve. The image is of a pea root nucleolus labelled with a probe to the ribosomal RNA genes.

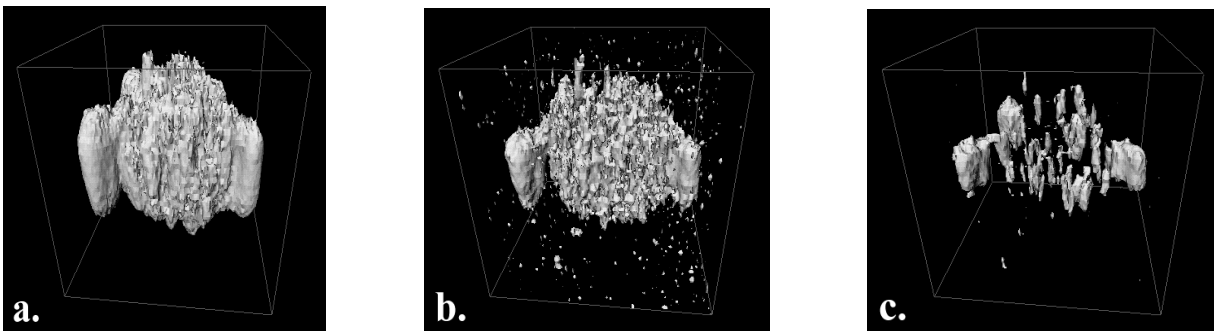


Figure 4. 3D Restoration and segmentation of a real optical microscopy image of a pea root nucleolus. Picture a- the blurred and noisy original image data after being rendering by Iris Explorer, Picture b- the original image in (a) after nonlinear restoration, and Picture c- image in (b) after segmentation by the Sieve.

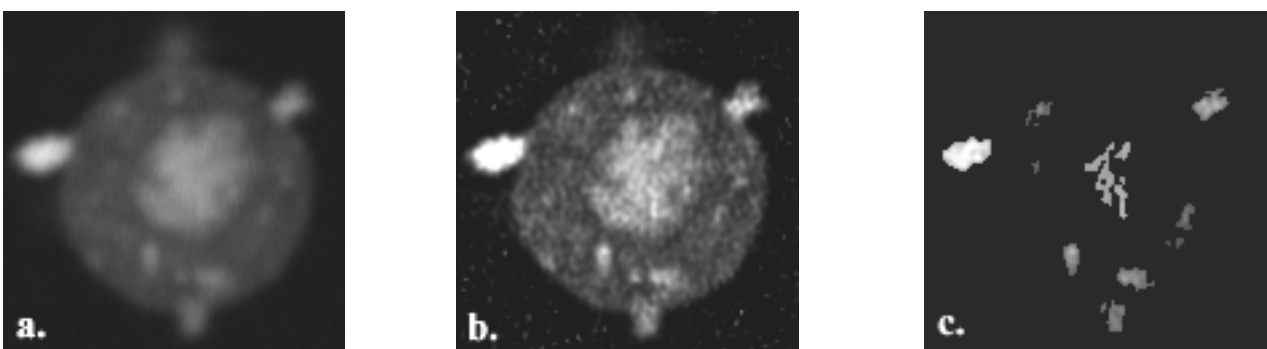


Figure 5. Restoration and segmentation of a single 2D slice from an original confocal image data set of 60 x128x128 voxels. Picture a - A single image slice of 128x128 pixels, Picture b - image (a) after nonlinear restoration, and Picture c- image (b) after segmentation by the Sieve. The image is of a pea nucleolus fluorescently labelled with antibody to the nucleolar protein fibrillarin.

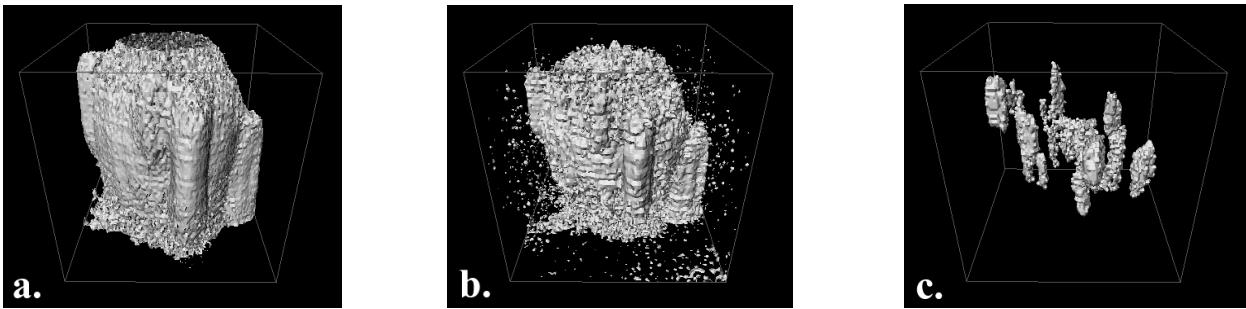


Figure 6. 3D Restoration and segmentation of a real optical microscopy image of a pea root nucleolus. Picture a- the blurred and noisy original image data after being rendered by Iris Explorer, Picture b- the original image in (a) after nonlinear restoration, and Picture c- Image in (b) after segmentation by the Sieve.

3. CONCLUSION

This paper has explored the synergism between sharpening 3D optical microscopy images by restoration and sieving. We presented a new methodology which combines nonlinear restoration and sieves to effectively segment volume objects within 3D optical microscopy images. For this combination to work, it is important that the images are first deblurred as we found that sieves can handle sharp edged objects very effectively. Smoothly changing objects, on the other hand, are not handled well by sieves because they spread over many scales in the granularity domain. The new methodology was applied to synthetic and real 3D confocal images, and was shown to perform effectively in producing good segmentation results.

REFERENCES

1. Rushforth, C. K. Chapter 1, Signal restoration, functional analysis and Fredholm integral equations of the first kind. Image recovery, theory and practice. Stark, H. : Academic Press, New York; 1987.
2. Youla, D.C. Generalised image restoration by the method of alternating orthogonal projections. IEEE Trans. Circ. Syst. 1978 25:695-702
3. Razaz, M.; Shaw, P. J.; Lee, R. A. 3D image restoration using a non-linear iterative deconvolution method. 3rd IMA Conf. on Maths in Signal Processing. ; 1992: 10-21.
4. Razaz, M.; Lee, R. A.; Shaw, P. J. A non-linear iterative least-squares algorithm for image restoration. : Proceedings IEEE Workshop on Nonlinear Signal Processing; 1993: 4-1, 4-6.
5. Razaz, M.; Lee, R. A.; Shaw, P. J. Computer modelling of point spread function for 3D image restoration. Signal processing VII: Theories & Applications. ; 1994: 303-306.
6. Razaz, M.; Lee, R. A. Comparison of an iterative deconvolution and Wiener filtering for image restoration. Image Processing: Math. Methods & Applic., Oxford Univ. Press, pp. 145-159, 1997.
7. Razaz, M.; Lee, R. A. Restoration of 3D real images using projection onto convex sets', Image Processing: Math. Methods & Applic., Oxford Univ. Press, , pp. 127-144, 1997.
8. Serra, J.; Salembier, P. Connected operators and pyramids. SPIE Proceedings on Image Algebra and Mathematical Morphology. 1993; 2030: 65-76.
9. Vincent, L. Morphological Grayscale Reconstruction in Image Analysis: Applications and Efficient Algorithms. IEEE Trans Image Processing. 1993; vol. 2: pp 176-201.
10. Bangham, J. A. Properties of a series of nested median filters, namely the datasieve. IEEE Trans. Signal Processing. 1993 1; vol. 41: pp 31-42.
11. Bangham, J. A.; Harvey, R. W.; Ling, P. D.; Aldridge, R. V. Nonlinear scale-space in many dimensions. European Conference on Computer Vision. : Kluwer; 1996 2; 1: 186:192.
12. Bangham, J. A.; Ling, P.; Young, R. Multiscale recursive medians, scale-space and sieve transforms with an inverse. IEEE Transactions on Image Processing. 1996 1; 5: 1043-1047.
13. Bosson, A.; Harvey, R. W.; Bangham, J. A. A comparison of linear and non-linear scale-space filters in noise. Signal Processing VIII. : Elsevier; 1996; 1: 1777-1781. ISBN: 88-86179-83.
14. Bangham, J. A.; Ling, P. D.; Harvey, R.; Aldridge, R. V. Nonlinear area and volume scale-space preserving filters. Journal of Electronic Imaging. 1996 3; 5: 283-299. ISSN: 1017-9909.
15. Vincent, L. Graphs and mathematical morphology. Signal Processing. 1989; 16: 365:388.
16. Pratt, K. P. Digital image processing. Wiley, New york, 1991.